

Highly Activated Terminal Carbon Monoxide Ligand in an Iron–Sulfur Cluster Model of FeMco with Intermediate Local Spin State at Fe

Linh N. V. Le, Justin P. Joyce, Paul H. Oyala, Serena DeBeer,* and Theodor Agapie*



Cite This: *J. Am. Chem. Soc.* 2024, 146, 5045–5050



Read Online

ACCESS |



Metrics & More



Article Recommendations



Supporting Information

ABSTRACT: Nitrogenases, the enzymes that convert N_2 to NH_3 , also catalyze the reductive coupling of CO to yield hydrocarbons. CO-coordinated species of nitrogenase clusters have been isolated and used to infer mechanistic information. However, synthetic FeS clusters displaying CO ligands remain rare, which limits benchmarking. Starting from a synthetic cluster that models a cubane portion of the FeMo cofactor (FeMoco), including a bridging carbyne ligand, we report a heterometallic tungsten–iron–sulfur cluster with a single terminal CO coordination in two oxidation states with a high level of CO activation ($\nu_{CO} = 1851$ and 1751 cm^{-1}). The local Fe coordination environment (2S, 1C, 1CO) is identical to that in the protein making this system a suitable benchmark. Computational studies find an unusual intermediate spin electronic configuration at the Fe sites promoted by the presence the carbyne ligand. This electronic feature is partly responsible for the high degree of CO activation in the reduced cluster.

Substrate activation at complex inorganic cofactors in enzyme active sites has raised fundamental questions about the role of the cluster structure on reactivity. For example, the challenging conversion of N_2 to NH_3 by nitrogenase enzymes occurs at FeMo cofactor (FeMoco) ($M = Mo, V$, or Fe), which comprises complex double cubane clusters with the MFe_7S_9C composition.^{1,2} Nitrogenases also catalyze the reductive coupling of CO to form hydrocarbons for $M = Mo$ and V .^{3,4} Despite interest in these transformations, the characterization of substrate-bound clusters is very rare, which limits insight into the site of small molecule activation and reaction mechanism.^{5–11} Only two CO-bound species of FeMoco and FeVco have been characterized structurally.^{9,10,12,13} Structural characterization of N_2 -derived species remains debated.^{14–16}

Synthetic models promise to facilitate a better understanding of the impact of cluster structure on substrate binding and level of activation.^{17–22} However, few examples of synthetic iron–sulfur clusters with terminal or bridging N_2 or CO ligands have been reported, many of which possess multiple CO ligands that drastically alter the electronic structure of the cluster and complicate comparisons to FeMoco (Figure 1).^{23–29} Only one type of FeS cluster with a single terminal CO ligand has been characterized, ligated by three carbene ligands.^{30,31}

Having accessed a partial synthetic analogue **1** of the cluster core of FeMoco displaying a μ_3 -carbyne ligand with the WFe_3S_3CR composition, where W is the isoelectronic analogue of Mo ,³² we targeted the coordination of nitrogenase substrates (Scheme 1).³³ Herein, we report the reactivity of **1** with isocyanides and CO, which affords an FeS cubane with a single terminal CO. We characterize this cluster in two oxidation states, which show a high level of CO activation, as observed in the low CO stretching frequency (1751 – 1851 cm^{-1}) by IR spectroscopy.

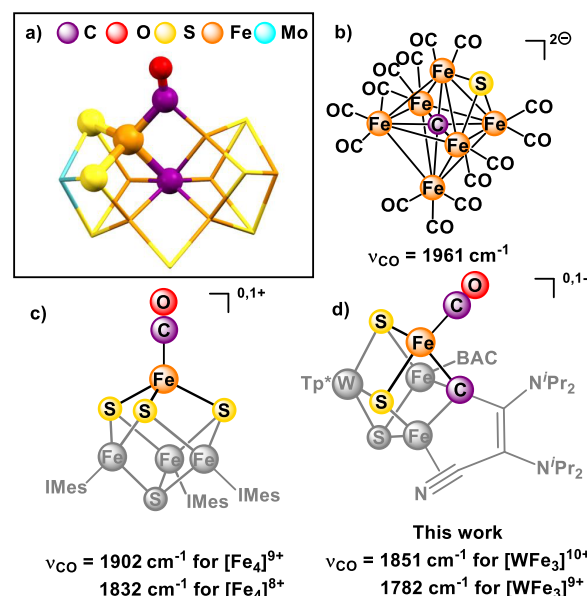


Figure 1. Structures of FeS clusters with CO coordination: (a) CO-bound FeMoco (PDB: 4TKV); (b) synthetic cluster with carbide ligand;^{26,27} (c) Fe_4S_4 cluster with a single terminal CO;³⁰ (d) present report. Local coordination sphere of Fe–CO moiety highlighted in (a), (c), and (d).

Received: October 27, 2023

Revised: January 29, 2024

Accepted: January 30, 2024

Published: February 15, 2024



Scheme 1. Syntheses of Clusters

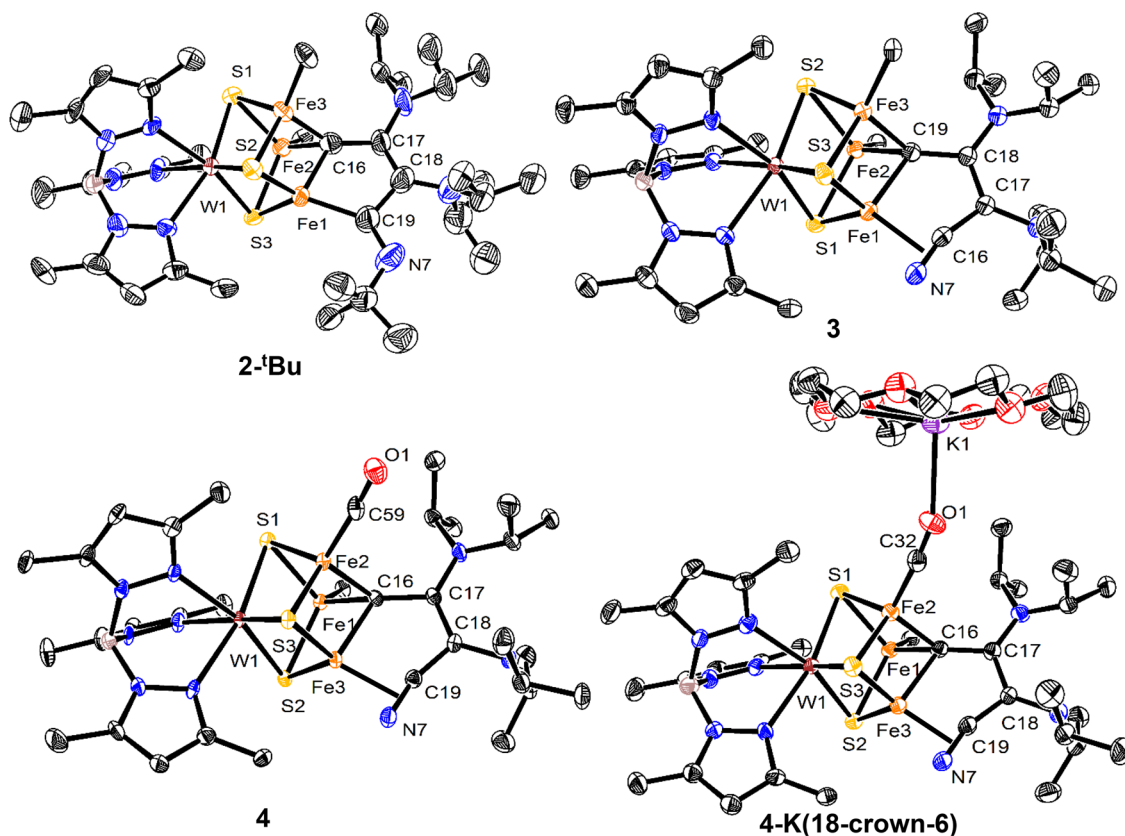
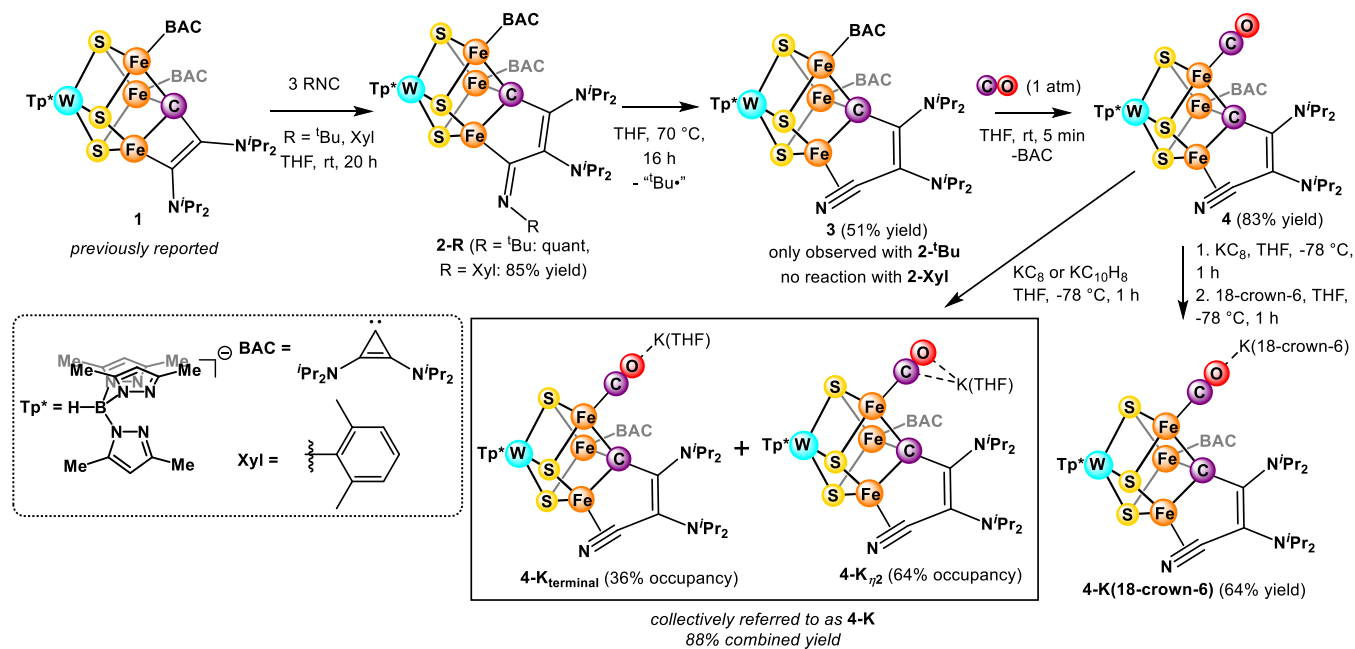


Figure 2. Crystal structures of 2-^tBu, 3, 4, and 4-K(18-crown-6). Ellipsoids are shown at 50% probability level. Hydrogen atoms, solvent molecules, and the BAC ligand, except for the carbene C, are omitted for clarity.

We employed isocyanides as isoelectronic analogues of CO and substrates of nitrogenase³⁴ that also allow for a more controlled reactivity. Treating 1 with ^tBuNC or XylNC (Xyl = 2,6-dimethylphenyl) gives 2-^tBu or 2-Xyl (Scheme 1), respectively, through the insertion of isocyanide into the Fe–C(vinyl) bond, which demonstrates rare examples of C–C

bond formation at an FeS cluster.^{35–38} Heating 2-^tBu in THF at 70 °C for 16 h leads to the formation of 3, where XRD and NMR studies are consistent with the loss of a ^tBu radical (leaving an η^2 -nitrile ligand).³⁹ While determining the protonation state of the N atom solely on the basis of XRD is inconclusive, the short C–N bond length of 1.205(6) Å

compared with ~ 1.25 Å for η^2 -iminoacyl (see the [Supporting Information](#) for additional literature comparison and support by ATR IR spectroscopy) is indicative of an η^2 -nitrile motif.⁴⁰ Loss of the ^tBu radical suggests a propensity for side-on nitrile binding, which is an intriguing observation in the context of the nitrogenase substrates displaying triple bonds, including N₂, acetylene, and isocyanides.⁴¹ The conversion from 2-^tBu to 3, which involves the loss of a ^tBu radical, formally represents one-electron oxidation of the WFe₃ metal core. In contrast to 2-^tBu, 2-Xyl is stable under the same conditions, which is consistent with a lower tendency to lose the more reactive aryl radical.⁴²

With 3 in hand, we explored reactions with CO. Cluster 3 reacts with 1 atm CO to form 4 within 5 min, which shows substitution of one bis(diisopropylamino)cyclopropenylidene (BAC) ligand with CO (83% yield, [Scheme 1](#)) in an uncommon instance of carbene lability.⁴³ The average Fe–C(μ_3) distance remains similar to 2-^tBu and 3 at 1.95 Å, but the range for the individual bond lengths increases to 1.88–2.00 Å (compared with 1.92–1.95 Å in 2-^tBu and 1.95–1.96 Å in 3), which suggests that the carbyne ligand, and potentially the carbide in FeMoco, has the ability to accommodate distinct electronic demands of different Fe centers through structural changes.⁴⁴ This is in contrast to spectroscopic studies suggesting that the central carbide serves to maintain the rigid core structure.^{8,45}

To the best of our knowledge, 4 is the only well-characterized example of a heterometallic MFe₃S₃(CR) cubane cluster bearing a single terminal CO ligand. This provides an opportunity for benchmarking the impact of structure and coordination environment relative to FeMoco. The THF solution IR spectrum of 4 displays a prominent peak at 1851 cm^{−1}, assigned as the C–O stretch ([Figure 3](#)) and confirmed by ¹³CO labeling ($\nu_{13\text{CO exp}} = 1807$ cm^{−1}, $\nu_{13\text{CO calc}} = 1810$ cm^{−1}), thereby suggesting highly activated CO.

To study the effects of cluster oxidation state on the level of CO activation, we reduced 4 with one equivalent of KC₈ or potassium naphthalenide to yield 4-K (*S* = 3/2, see the [Supporting Information](#)) ([Scheme 1](#)). As expected, the CO bond length increases upon reduction from 1.15(1) to 1.198(3) Å. The solution IR spectrum of 4-K shows two C–O bands at 1794 and 1751 cm^{−1} ([Figure 3](#)), which is consistent with the crystal structure of 4-K displaying CO–K⁺ interactions disordered over two positions: terminal (36% occupancy) (assigned as 4-K_{terminal}) and η^2 (64% occupancy) (assigned as 4-K _{η^2}). These isomers are collectively referred to as 4-K. Chelation of K⁺ with 18-crown-6 results in the formation of 4-K(18-crown-6). XRD shows that the K⁺ ion is present in only one location and interacts end-on with the O atom of CO ([Figure 2](#)). In agreement, the IR spectrum shows a single band at 1782 cm^{−1} ([Figure 3](#); $\nu_{13\text{CO exp}} = 1740$ cm^{−1}; $\nu_{13\text{CO calc}} = 1742$ cm^{−1}). The same band is observed upon treatment with [2.2.2]cryptand, thereby suggesting that the K⁺ ion in 4-K(18-crown-6) does not impact CO activation substantially.⁴⁶

Both 4-K and 4-K(18-crown-6) exhibit highly activated CO ligands coordinated to Fe in a terminal fashion. The interaction with K⁺ in different binding modes affects the level of CO activation in the 1794 and 1751 cm^{−1} range. Previous computational work describes a semibridging CO ligand at Fe2 in FeMoco with a frequency of 1718 cm^{−1},⁴⁷ very close to that assigned to the bridging CO in lo-CO at 1715 cm^{−1}.⁴⁸ This is slightly lower than the typical values observed for μ_2 -

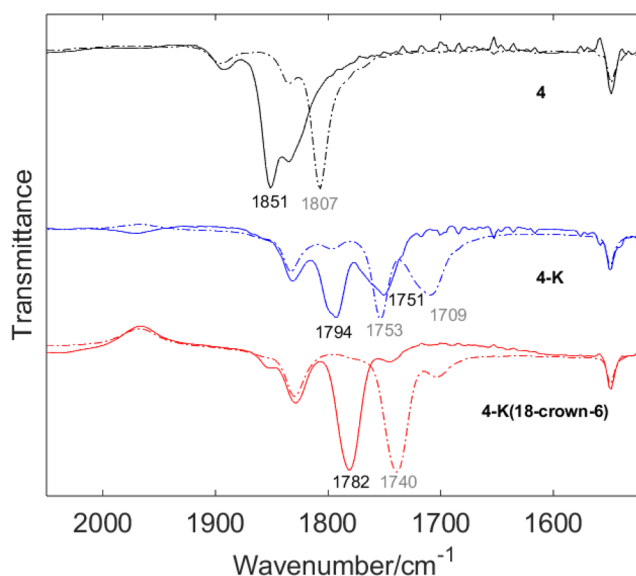


Figure 3. IR spectra of 4, 4-K, and 4-K(18-crown-6) (THF solution) with ν_{CO} values shown. Dashed spectra correspond to ¹³CO-labeled species with $\nu_{13\text{CO}}$ in gray. The feature at 1830 cm^{−1} unchanged upon ¹³CO labeling is assigned to BAC.

CO ligands, which lie in the 1720–1850 cm^{−1} range.⁴⁹ Hydrogen bonding between the carbonyl oxygen and the nearby His195 residue is proposed to further activate CO.⁴⁷ Similarly, in 4-K, the K⁺ cation can play the same role as the hydrogen bonding network and lower the C–O stretching frequency. Nevertheless, ν_{CO} values below 1800 cm^{−1} are unprecedented for FeS clusters. For comparison, the CO adducts of *N*-heterocyclic carbene (NHC)-supported Fe₄S₄ clusters reported by Suess and co-workers display C–O stretching frequencies of 1832 cm^{−1} for the [Fe₄S₄]⁰ and 1902 cm^{−1} for the [Fe₄S₄]⁺ states.³⁰ The local coordination environment at each Fe (FeS₂C in 4 and 4-K and FeS₃ in [Fe₄S₄]^{+,0}) and oxidation state distribution between different metal sites can contribute to the level of diatomic activation.^{30,50,51}

In order to understand the electronic structure origin of the profound CO activation in these clusters, we employed computational methods using broken symmetry density functional theory (BS-DFT). Our computational procedure detailed in the [Supporting Information](#) accurately assigns the geometric, Mössbauer, and vibrational properties of 4 and 4-K. Here, we highlight the impact of the carbyne, W³⁺ center, and a K⁺ counteranion with respect to the strong CO activation in 4-K.

The carbyne has three anionic lone pairs oriented along the Fe-bonding axes in its μ_3 -binding mode. The localized orbitals characterize the carbyne lone pairs as σ -donors that stabilize the intermediate spin (IS) state of the three formal Fe²⁺ (*S* = 1) centers. Observing the IS state at the Fe sites that do not bind CO suggests that it is an innate property of the μ_3 -carbyne ligand. The IS state in Fe²⁺ centers give full occupation of its π -backbonding orbitals, consistent with the increased CO activation in 4-K. In agreement, hyperfine sublevel correlation (HYSCORE) spectra of 4-K(¹³CO) show small hyperfine coupling to the ¹³C center of CO [$A(^{13}\text{C}) = [-0.5, 1.0, -0.5]$ MHz; see the [Supporting Information](#)]. A partially occupied Fe–CO backbonding orbital is expected to result in larger coupling.^{5,52,53} In comparison, Fe centers in FeS clusters are

routinely assigned as high-spin because of their weak ligand field environment, such as the $S = 3/2$ state assigned to the CO-bound Fe^{1+} by Suess and co-workers.³⁰

Furthermore, the Fe centers are preferentially ferromagnetically coupled, which results in the equal delocalization of two electrons among the three Fe atoms (Figure 4). This formally

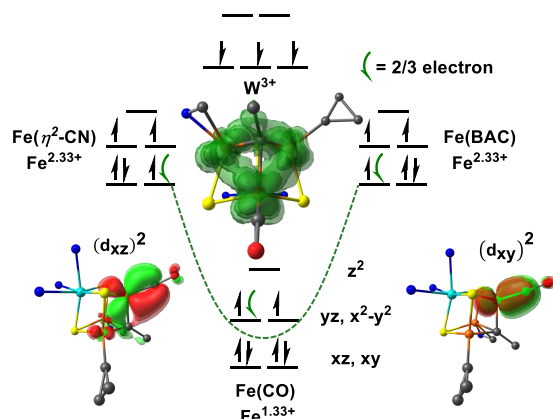


Figure 4. Local oxidation and spin states of the metal centers of 4^- ($S = 3/2$) with respect to the Mulliken spin population of their PM-localized orbitals (Figures S34–36). The curved green arrow denotes a pair of electrons that are equally delocalized among the Fe centers (illustrated in the inset) with respect to its localized spin density. The degenerate Fe–CO π -bonding interactions are shown at the bottom with respect to their localized orbitals.

lowers the oxidation state of the CO-bound Fe site from its formal 2+ to 1.33+ charge and proportionately increases the other Fe centers to 2.33+; their resonance states are illustrated in the [Supporting Information](#). This is analogous to the net $\text{Fe}^{2.5+}$ oxidation state resulting from the equal delocalization of one electron between two Fe sites in formal $\text{Fe}^{2+}\text{--Fe}^{3+}$ dimers.⁵⁴ This pairwise delocalization supports a reduced state at the CO-bound center that is otherwise inaccessible under biological conditions. Similarly, redox disproportionation has been proposed in previously reported $[\text{Fe}_6(\mu_6\text{-C})(\text{CO})_{18}]$ and $\text{Fe}_4\text{S}_4(\text{CO})(\text{IMes})_3$ clusters, where Fe sites of different oxidation states are within close proximity.^{30,55}

The anionic charge of 4^- supports strong noncovalent interactions with its counteranion. The geometry optimization of **4-K** preferentially binds K^+ in an η^2 -conformation with respect to the CO bond. The calculated CO stretching frequency decreases from 1800 cm^{-1} without K^+ to 1756 cm^{-1} , which is consistent with the distinct vibrational modes observed in the IR spectrum of **4-K**. The electronic structure of the cluster is not impacted by K coordination, thereby suggesting that it is a purely ionic interaction that stabilizes the π -bonding of the CO ligand.

The CO lone pair can overlap with orbitals arising from the Fe–W interaction assigned as purely covalent in 4^- on the basis of the localized orbitals (see Figure S34 for a graphical representation). The Fe–W covalent interaction redistributes electron density between the metal centers promoting the electrostatic attraction with the CO lone pair and consequently also enhances the π^* -backbonding discussed above.^{56,57} The other Fe centers exhibit bonding characters that are intermediate of a covalent and magnetic interaction, analogous to bonding properties detailed in the Mo^{3+} heteroatom of FeMoCo .^{58,59} In contrast, this is not observed for the cluster reported by Suess and co-workers³⁰ because of the

comparatively weak bonding interactions between Fe sites. Overall, these factors contribute to the stronger CO activation in 4^- compared with these reported clusters with an average metal oxidation state of 2+, despite the higher average metal oxidation state of 2.25+ in 4^- .³⁰

In summary, we have reported a series of heterometallic $\text{WFe}_3\text{S}_3\text{CR}$ cubanes and demonstrated several types of organometallic transformations and binding modes that are rare for iron–sulfur clusters. These compounds show C–C coupling, along with side-on binding of an organic nitrile moiety at one Fe site. Furthermore, we characterized the first example of a heterometallic iron–sulfur cluster with a single terminally bound, highly activated CO ligand in two oxidation states. Computation suggests an unusual carbyne-promoted intermediate spin electronic configuration at all Fe sites, along with a low oxidation state of 1.33+ for Fe(CO) in 4^- . This electron configuration affords full occupancy of the two π -back-bonding orbitals to CO, which are responsible for the high level of CO activation in the reduced clusters. The negative charge of the cluster and the metal–metal covalency were found computationally to also impact CO activation. These findings provide a set of parameters to evaluate in future studies for the conversion of substrates in nitrogenase.

■ ASSOCIATED CONTENT

SI Supporting Information

The Supporting Information is available free of charge at <https://pubs.acs.org/doi/10.1021/jacs.3c12025>.

General methods, synthetic procedures, product isolation and characterization, NMR spectra, structural information, and computational methods ([PDF](#))

Accession Codes

CCDC 2130433–2130434, 2130436, 2233067–2233070, and 2233072 contain the supplementary crystallographic data for this paper. These data can be obtained free of charge via www.ccdc.cam.ac.uk/data_request/cif, or by emailing data_request@ccdc.cam.ac.uk, or by contacting The Cambridge Crystallographic Data Centre, 12 Union Road, Cambridge CB2 1EZ, UK; fax: +44 1223 336033.


■ AUTHOR INFORMATION

Corresponding Authors

Serena DeBeer – *Max Planck Institute for Chemical Energy Conversion, 45470 Mülheim an der Ruhr, Germany;*

 orcid.org/0000-0002-5196-3400;


Email: serena.debeer@cec.mpg.de

Theodor Agapie – Division of Chemistry and Chemical Engineering, California Institute of Technology, Pasadena, California 91125, United States;  orcid.org/0000-0002-9692-7614; Email: agapie@caltech.edu

Authors

Linh N. V. Le – *Division of Chemistry and Chemical Engineering, California Institute of Technology, Pasadena, California 91125, United States*

Justin P. Joyce – Max Planck Institute for Chemical Energy
Conversion, 45470 Mülheim an der Ruhr, Germany

Paul H. Oyala – Division of Chemistry and Chemical Engineering, California Institute of Technology, Pasadena, California 91125, United States;  orcid.org/0000-0002-8761-4667

Complete contact information is available at:

<https://pubs.acs.org/10.1021/jacs.3c12025>

Notes

The authors declare no competing financial interest.

ACKNOWLEDGMENTS

We are grateful to the National Institutes of Health (R01-GM102687B to T.A.) and the Humboldt Foundation for funding for T.A. (a Bessel Research Award) and J.P.J. We thank the Beckman Institute and the Dow Next Generation Grant for instrumentation support. Michael Takase and Lawrence Henling are thanked for assistance with crystallography. J.P.J. and S.D. acknowledge the Max Planck Society for funding.

REFERENCES

- (1) Spatzal, T.; Schlesier, J.; Burger, E.-M.; Sippel, D.; Zhang, L.; Andrade, S. L. A.; Rees, D. C.; Einsle, O. Nitrogenase FeMoco Investigated by Spatially Resolved Anomalous Dispersion Refinement. *Nat. Commun.* **2016**, *7* (1), 10902.
- (2) Sippel, D.; Einsle, O. The Structure of Vanadium Nitrogenase Reveals an Unusual Bridging Ligand. *Nat. Chem. Biol.* **2017**, *13* (9), 956–960.
- (3) Hu, Y.; Lee, C. C.; Ribbe, M. W. Extending the Carbon Chain: Hydrocarbon Formation Catalyzed by Vanadium/Molybdenum Nitrogenases. *Science* **2011**, *333* (6043), 753.
- (4) Lee, C. C.; Hu, Y.; Ribbe, M. W. Catalytic Reduction of CN[−], CO, and CO₂ by Nitrogenase Cofactors in Lanthanide-Driven Reactions. *Angew. Chem., Int. Ed.* **2015**, *54* (4), 1219–1222.
- (5) Lee, H.-L.; Cameron, L. M.; Hales, B. J.; Hoffman, B. M. CO Binding to the FeMo Cofactor of CO-Inhibited Nitrogenase: 13CO and 1H Q-Band ENDOR Investigation. *J. Am. Chem. Soc.* **1997**, *119* (42), 10121–10126.
- (6) George, S. J.; Ashby, G. A.; Wharton, C. W.; Thorneley, R. N. F. Time-Resolved Binding of Carbon Monoxide to Nitrogenase Monitored by Stopped-Flow Infrared Spectroscopy. *J. Am. Chem. Soc.* **1997**, *119* (27), 6450–6451.
- (7) Davis, L. C.; Henzl, M. T.; Burris, R. H.; Orme-Johnson, W. H. Iron-Sulfur Clusters in the Molybdenum-Iron Protein Component of Nitrogenase. Electron Paramagnetic Resonance of the Carbon Monoxide Inhibited State. *Biochemistry* **1979**, *18* (22), 4860–4869.
- (8) Pérez-González, A.; Yang, Z.-Y.; Lukoyanov, D. A.; Dean, D. R.; Seefeldt, L. C.; Hoffman, B. M. Exploring the Role of the Central Carbide of the Nitrogenase Active-Site FeMo-Cofactor through Targeted 13C Labeling and ENDOR Spectroscopy. *J. Am. Chem. Soc.* **2021**, *143* (24), 9183–9190.
- (9) Rohde, M.; Grunau, K.; Einsle, O. CO Binding to the FeV Cofactor of CO-Reducing Vanadium Nitrogenase at Atomic Resolution. *Angew. Chem., Int. Ed.* **2020**, *59* (52), 23626–23630.
- (10) Rohde, M.; Laun, K.; Zebger, I.; Stripp, S. T.; Einsle, O. Two Ligand-Binding Sites in CO-Reducing V Nitrogenase Reveal a General Mechanistic Principle. *Sci. Adv.* **2021**, *7* (22), No. eabg4474.
- (11) Van Stappen, C.; Decamps, L.; Cutsail, G. E.; Bjornsson, R.; Henthorn, J. T.; Birrell, J. A.; DeBeer, S. The Spectroscopy of Nitrogenases. *Chem. Rev.* **2020**, *120* (12), 5005–5081.
- (12) Spatzal, T.; Perez, K. A.; Einsle, O.; Howard, J. B.; Rees, D. C. Ligand Binding to the FeMo-Cofactor: Structures of CO-Bound and Reactivated Nitrogenase. *Science* **2014**, *345* (6204), 1620.
- (13) Buscagan, T. M.; Perez, K. A.; Maggiolo, A. O.; Rees, D. C.; Spatzal, T. Structural Characterization of Two CO Molecules Bound to the Nitrogenase Active Site. *Angew. Chem., Int. Ed.* **2021**, *60* (11), 5704–5707.
- (14) Kang, W.; Lee, C. C.; Jasniowski, A. J.; Ribbe, M. W.; Hu, Y. Structural Evidence for a Dynamic Metallocofactor during N₂ Reduction by Mo-Nitrogenase. *Science* **2020**, *368* (6497), 1381.
- (15) Peters, J. W.; Einsle, O.; Dean, D. R.; DeBeer, S.; Hoffman, B. M.; Holland, P. L.; Seefeldt, L. C. Comment on “Structural Evidence for a Dynamic Metallocofactor during N₂ Reduction by Mo-Nitrogenase. *Science* **2021**, *371* (6530), No. eabe5481.
- (16) Kang, W.; Lee, C. C.; Jasniowski, A. J.; Ribbe, M. W.; Hu, Y. Response to Comment on “Structural Evidence for a Dynamic Metallocofactor during N₂ Reduction by Mo-Nitrogenase. *Science* **2021**, *371* (6530), No. eabe5856.
- (17) McSkimming, A.; Suess, D. L. M. Dinitrogen Binding and Activation at a Molybdenum–Iron–Sulfur Cluster. *Nat. Chem.* **2021**, *13* (7), 666–670.
- (18) Sridharan, A.; Brown, A. C.; Suess, D. L. M. A Terminal Imido Complex of an Iron–Sulfur Cluster. *Angew. Chem., Int. Ed.* **2021**, *60* (23), 12802–12806.
- (19) Anderton, K. J.; Knight, B. J.; Rheingold, A. L.; Abboud, K. A.; García-Serres, R.; Murray, L. J. Reactivity of Hydride Bridges in a High-Spin [Fe₃(μ-H)₃]³⁺ Cluster: Reversible H₂/CO Exchange and Fe–H/B–F Bond Metathesis. *Chem. Sci.* **2017**, *8* (5), 4123–4129.
- (20) Arnett, C. H.; Agapie, T. Activation of an Open Shell, Carbyne-Bridged Diiron Complex Toward Binding of Dinitrogen. *J. Am. Chem. Soc.* **2020**, *142* (22), 10059–10068.
- (21) Arnett, C. H.; Bogacz, I.; Chatterjee, R.; Yano, J.; Oyala, P. H.; Agapie, T. Mixed-Valent Diiron μ-Carbyne, μ-Hydride Complexes: Implications for Nitrogenase. *J. Am. Chem. Soc.* **2020**, *142* (44), 18795–18813.
- (22) Ohki, Y.; Munakata, K.; Matsuoka, Y.; Hara, R.; Kachi, M.; Uchida, K.; Tada, M.; Cramer, R. E.; Sameera, W. M. C.; Takayama, T.; Sakai, Y.; Kuriyama, S.; Nishibayashi, Y.; Tanifuji, K. Nitrogen Reduction by the Fe Sites of Synthetic [Mo₃S₄Fe] Cubes. *Nature* **2022**, *607* (7917), 86–90.
- (23) Tyson, M. A.; Coucouvanis, D. New Fe/Mo/S Clusters with MoFe₃S₃ Cuboidal Cores Similar to the One in the Fe/Mo Cofactor of Nitrogenase. Synthesis and Structural Characterization of the (C14-Cat)MoFe₃S₃(PEt₃)₂(CO)₆ and (C14-Cat)Mo(O)Fe₃S₃(PEt₃)₃(CO)₅ Clusters. *Inorg. Chem.* **1997**, *36* (18), 3808–3809.
- (24) Han, J.; Beck, K.; Ockwig, N.; Coucouvanis, D. Synthetic Analogs for the MoFe₃S₃ Subunit of the Nitrogenase Cofactor: Structural Features Associated with the Total Number of Valence Electrons and the Possible Role of M–M and Multiple M–S Bonding in the Function of Nitrogenase. *J. Am. Chem. Soc.* **1999**, *121* (44), 10448–10449.
- (25) Coucouvanis, D.; Han, J.; Moon, N. Synthesis and Characterization of Sulfur-Voided Cubanes. Structural Analogues for the MoFe₃S₃ Subunit in the Nitrogenase Cofactor. *J. Am. Chem. Soc.* **2002**, *124* (2), 216–224.
- (26) Joseph, C.; Cobb, C. R.; Rose, M. J. Single-Step Sulfur Insertions into Iron Carbide Carbonyl Clusters: Unlocking the Synthetic Door to FeMoco Analogues. *Angew. Chem., Int. Ed.* **2021**, *60* (7), 3433–3437.
- (27) Liu, L.; Rauchfuss, T. B.; Woods, T. J. Iron Carbide–Sulfide Carbonyl Clusters. *Inorg. Chem.* **2019**, *58* (13), 8271–8274.
- (28) Brunner, H.; Janietz, N.; Wachter, J.; Zahn, T.; Ziegler, M. L. Novel MoFeS Clusters from [(C₆Me₅)₂Mo₂S₄] and Fe(CO)₅ or Fe₂(CO)₉. *Angew. Chem., Int. Ed. Engl.* **1985**, *24* (2), 133–135.
- (29) Joseph, C.; Shupp, J. P.; Cobb, C. R.; Rose, M. J. Construction of Synthetic Models for Nitrogenase-Relevant NiFe Biogenesis Intermediates and Iron-Carbide-Sulfide Clusters. *Catalysts* **2020**, *10* (11), 1317.
- (30) Brown, A. C.; Thompson, N. B.; Suess, D. L. M. Evidence for Low-Valent Electronic Configurations in Iron–Sulfur Clusters. *J. Am. Chem. Soc.* **2022**, *144* (20), 9066–9073.
- (31) Brown, A. C.; Suess, D. L. M. An Iron–Sulfur Cluster with a Highly Pyramidalized Three-Coordinate Iron Center and a Negligible Affinity for Dinitrogen. *J. Am. Chem. Soc.* **2023**, *145* (36), 20088–20096.
- (32) Holm, R. H.; Solomon, E. I.; Majumdar, A.; Tenderholt, A. Comparative Molecular Chemistry of Molybdenum and Tungsten and Its Relation to Hydroxylase and Oxotransferase Enzymes. *Coord. Chem. Rev.* **2011**, *255* (9), 993–1015.
- (33) Le, L. N. V.; Bailey, G. A.; Scott, A. G.; Agapie, T. Partial Synthetic Models of FeMoco with Sulfide and Carbyne Ligands:

Effect of Interstitial Atom in Nitrogenase Active Site. *Proc. Natl. Acad. Sci. U.S.A.* **2021**, *118* (49), No. e2109241118.

(34) Seefeldt, L. C.; Yang, Z.-Y.; Duval, S.; Dean, D. R. Nitrogenase Reduction of Carbon-Containing Compounds. *Biochim. Biophys. Acta - Bioenerg.* **2013**, *1827* (8), 1102–1111.

(35) Brown, A. C.; Suess, D. L. M. Reversible Formation of Alkyl Radicals at [Fe₄S₄] Clusters and Its Implications for Selectivity in Radical SAM Enzymes. *J. Am. Chem. Soc.* **2020**, *142* (33), 14240–14248.

(36) Lichtenberg, C.; Garcia Rubio, I.; Viciu, L.; Adelhardt, M.; Meyer, K.; Jeschke, G.; Grützmacher, H. A Low-Valent Iron Imido Heterocubane Cluster: Reversible Electron Transfer and Catalysis of Selective C–C Couplings. *Angew. Chem., Int. Ed.* **2015**, *54* (44), 13012–13017.

(37) Muñoz, S. B.; Daifuku, S. L.; Brennessel, W. W.; Neidig, M. L. Isolation, Characterization, and Reactivity of Fe₈Me₁₂ – : Kochi's S = 1/2 Species in Iron-Catalyzed Cross-Couplings with MeMgBr and Ferric Salts. *J. Am. Chem. Soc.* **2016**, *138* (24), 7492–7495.

(38) Bradley, J. S.; Ansell, G. B.; Hill, E. W. Homogeneous Carbon Monoxide Hydrogenation on Multiple Sites: A Dissociative Pathway to Oxygenates. *J. Am. Chem. Soc.* **1979**, *101* (24), 7417–7419.

(39) Vacuum transfer of volatiles from the synthesis of 3 allows for the identification of isobutane and isobutene. See the [Supporting Information](#) for more information.

(40) Lis, E. C.; Delafuente, D. A.; Lin, Y.; Mocella, C. J.; Todd, M. A.; Liu, W.; Sabat, M.; Myers, W. H.; Harman, W. D. The Uncommon Reactivity of Dihapto-Coordinated Nitrile, Ketone, and Alkene Ligands When Bound to a Powerful π -Base. *Organometallics* **2006**, *25* (21), 5051–5058.

(41) Brown, A. C.; Suess, D. L. M. Valence Localization in Alkyne and Alkene Adducts of Synthetic [Fe₄S₄]⁺ Clusters. *Inorg. Chem.* **2023**, *62*, 1911.

(42) Peters, J. C.; Johnson, A. R.; Odom, A. L.; Wanandi, P. W.; Davis, W. M.; Cummins, C. C. Assembly of Molybdenum/Titanium μ -Oxo Complexes via Radical Alkoxide C–O Cleavage. *J. Am. Chem. Soc.* **1996**, *118* (42), 10175–10188.

(43) Crudden, C. M.; Allen, D. P. Stability and Reactivity of N-Heterocyclic Carbene Complexes. *Coord. Chem. Rev.* **2004**, *248* (21), 2247–2273.

(44) Rittle, J.; Peters, J. C. Fe–N₂/CO Complexes That Model a Possible Role for the Interstitial C Atom of FeMo-Cofactor (FeMoco). *Proc. Natl. Acad. Sci. U.S.A.* **2013**, *110* (40), 15898.

(45) Lukyanov, D. A.; Yang, Z.-Y.; Pérez-González, A.; Raugei, S.; Dean, D. R.; Seefeldt, L. C.; Hoffman, B. M. ¹³C ENDOR Characterization of the Central Carbon within the Nitrogenase Catalytic Cofactor Indicates That the CFe₆ Core Is a Stabilizing “Heart of Steel.” *J. Am. Chem. Soc.* **2022**, *144* (40), 18315–18328.

(46) Joseph, C.; Kuppuswamy, S.; Lynch, V. M.; Rose, M. J. Fe₅Mo Cluster with Iron-Carbide and Molybdenum-Carbide Bonding Motifs: Structure and Selective Alkyne Reductions. *Inorg. Chem.* **2018**, *57* (1), 20–23.

(47) Spiller, N.; Bjornsson, R.; DeBeer, S.; Neese, F. Carbon Monoxide Binding to the Iron–Molybdenum Cofactor of Nitrogenase: A Detailed Quantum Mechanics/Molecular Mechanics Investigation. *Inorg. Chem.* **2021**, *60* (23), 18031–18047.

(48) Gee, L. B.; Myers, W. K.; Nack-Lehman, P. A.; Scott, A. D.; Yan, L.; George, S. J.; Dong, W.; Dapper, C. H.; Newton, W. E.; Cramer, S. P. Nitrogenase Chemistry at 10 K—Phototautomerization and Recombination of CO-Inhibited α -H195Q Enzyme. *Inorg. Chem.* **2022**, *61* (30), 11509–11513.

(49) Crabtree, R. H. Chapter 4: Carbonyls, Phosphines, and Substitution. In *The Organometallic Chemistry of the Transition Metals*; John Wiley & Sons, Inc.: Hoboken, NJ, 2004; pp 98–133.

(50) Arnett, C. H.; Kaiser, J. T.; Agapie, T. Remote Ligand Modifications Tune Electronic Distribution and Reactivity in Site-Differentiated, High-Spin Iron Clusters: Flipping Scaling Relationships. *Inorg. Chem.* **2019**, *58* (23), 15971–15982.

(51) Arnett, C. H.; Chalkley, M. J.; Agapie, T. A Thermodynamic Model for Redox-Dependent Binding of Carbon Monoxide at Site-

Differentiated, High Spin Iron Clusters. *J. Am. Chem. Soc.* **2018**, *140* (16), 5569–5578.

(52) Bailey, G. A.; Buss, J. A.; Oyala, P. H.; Agapie, T. Terminal, Open-Shell Mo Carbide and Carbyne Complexes: Spin Delocalization and Ligand Noninnocence. *J. Am. Chem. Soc.* **2021**, *143* (33), 13091–13102.

(53) Rao, G.; Britt, R. D. Electronic Structure of Two Catalytic States of the [FeFe] Hydrogenase H-Cluster As Probed by Pulse Electron Paramagnetic Resonance Spectroscopy. *Inorg. Chem.* **2018**, *57* (17), 10935–10944.

(54) Soncini, A.; Mallah, T.; Chibotaru, L. F. Molecular Spintronics in Mixed-Valence Magnetic Dimers: The Double-Exchange Blockade Mechanism. *J. Am. Chem. Soc.* **2010**, *132* (23), 8106–8114.

(55) Kuppuswamy, S.; Wofford, J. D.; Joseph, C.; Xie, Z.-L.; Ali, A. K.; Lynch, V. M.; Lindahl, P. A.; Rose, M. J. Structures, Interconversions, and Spectroscopy of Iron Carbonyl Clusters with an Interstitial Carbide: Localized Metal Center Reduction by Overall Cluster Oxidation. *Inorg. Chem.* **2017**, *56* (10), 5998–6012.

(56) Loipersberger, M.; Mao, Y.; Head-Gordon, M. Variational Forward–Backward Charge Transfer Analysis Based on Absolutely Localized Molecular Orbitals: Energetics and Molecular Properties. *J. Chem. Theory Comput.* **2020**, *16* (2), 1073–1089.

(57) Lupinetti, A. J.; Fau, S.; Frenking, G.; Strauss, S. H. Theoretical Analysis of the Bonding between CO and Positively Charged Atoms. *J. Phys. Chem. A* **1997**, *101* (49), 9551–9559.

(58) Bjornsson, R.; Lima, F. A.; Spatzal, T.; Weyhermüller, T.; Glatzel, P.; Bill, E.; Einsle, O.; Neese, F.; DeBeer, S. Identification of a Spin-Coupled Mo(III) in the Nitrogenase Iron–Molybdenum Cofactor. *Chem. Sci.* **2014**, *5* (8), 3096–3103.

(59) Bjornsson, R.; Neese, F.; Schrock, R. R.; Einsle, O.; DeBeer, S. The Discovery of Mo(III) in FeMoco: Reuniting Enzyme and Model Chemistry. *J. Biol. Inorg. Chem.* **2015**, *20* (2), 447–460.